NEW APPROACH TO HIGH ENERGY
$SU_{2L} \times U_1$ RADIATIVE CORRECTIONS*

B. F. L. WARD

Stanford Linear Accelerator Center
Stanford University, Stanford, California, 94309

and

Department of Physics and Astronomy
The University of Tennessee, Knoxville, Tennessee 37996–1200

ABSTRACT

We present a new approach to $SU_{2L} \times U_1$ radiative corrections at high energies. Our approach is based on the infrared summation methods of Yennie, Frautschi and Suura, taken together with the Weinberg–'t Hooft renormalization group equation. Specific processes which have been realized via explicit Monte Carlo algorithms are $e^+e^- \rightarrow f\bar{f} + n(\gamma)$, $f = \mu, \tau, d, s, u, c, b$ or t and $e^+e^- \rightarrow e^+e^- + n(\gamma)$, where $n(\gamma)$ denotes multiple photon emission on an event-by-event basis. Exemplary Monte Carlo data are presented.

Invited talk presented at the XXVIII Cracow School of Theoretical Physics,
Zakopane, Poland, May 31–June 10, 1988

I. INTRODUCTION

As we and others[1] have described elsewhere, the primary objective of SLC, LEP, HERA, TLC and CLIC is to probe the limits of the $SU_{2L} \times U_1 \times SU_3^c$ standard model. This model appears to have no known contradiction with observation. Accordingly, it is indeed appropriate to determine the limits, if any, of its applicability by probing deeper into the nature of its forces. One way of probing more deeply in this connection is to scatter standard model particles at higher and higher energies. The achievement of such higher energies is the *raison d'etre* of the new accelerators.

These lepton-lepton and lepton-hadron colliders, then, hope to probe the limits of applicability of the standard model to the processes $e^+e^- \rightarrow X$, $e^{\pm}p \rightarrow X'$, etc., at very high energies. Such probes will provide information on the precise values of some of the as yet approximately known standard model coupling parameters and masses, such as $\sin^2 \theta_W$ and M_{Z°. Alternatively, one can view the standard model as specified by α, G_μ, M_{Z°, m_H, $\{m_f\}$ and Λ_{QCD}, where m_H is the rest mass of the as yet unobserved physical Higgs particle and $\{m_f\}$ are the standard model fermion rest masses (for the purposes of our discussion, the t–quark should be included as a *"known"* standard model fermion). New physics, such as SUSY, may enlarge this parameter set so that high energy lepton-lepton and lepton-hadron colliders may reveal the inadequacy of the standard model by producing evidence for super-particles, for example.

More precisely, one may summarize the nature of the lepton-lepton and lepton-hadron probes as follows. At the SLC and LEP, one hopes to effect precision measurements in Z° physics[1] of such quantities as M_{Z°, Γ_{Z°, A_{LR}, ...; the consequence will be restrictions on the number of light ν's, constraints on possible new heavy particles, etc. (For more detailed discussion of such matters, see Refs. 1.) Similarly, precision measurements of W^+W^- pair production at TLC and CLIC would allow one to probe the gauge structure of the $SU_{2L} \times U_1$ theory, for example. Precise measurements at HERA of the structure functions of the proton over a large Q^2 range would allow tests of QCD and may also reveal *"new physics,"* for example. What is clear about all such scenarios is

that they require precision radiative corrections in order to realize their main discovery potential in a complete way.

The question naturally arises as to what, then, is the current state of precision $SU_{2L} \times U_1$ radiative corrections at high energies. Regarding the SLC–LEP type scenario, we note that the level of precision required in the radiative corrections for the type of phenomena to be pursued[1,2] may be taken to be $\lesssim .3\%$. We then call attention to the recent improvements[3] of the original work of Jackson and Scharre[4] on the total cross section in $e^+e^- \to X$ by Kuraev and Fadin, Berends et al., Nicrosini and Trentadue, Cahn, Greco, Altarelli and Martinelli, and Lynn et al. A detailed comparison of the results of such analyses is given in Ref. 5, where it is shown that the former four are all consistent with one another at the level of $\lesssim 1\%$. The key improvement of these authors over the original work of Jackson and Scharre is the inclusion of the higher order renormalization of the Jackson–Scharre kernel substitution $1 + t(1/x)_+ \to tx^{t-1}$ with the attendant omission of the delta function contribution to the Jackson–Scharre photon spectrum at $x = 0$. Here, we use the conventional notation x for the bremsstrahlung photon energy in units of one-half of the total e^+e^- energy $\sqrt{s}$ in the center-of-momentum frame, and $t \equiv (2\alpha/\pi)[\ell n(s/m_e^2) - 1]$, where m_e is the electron rest mass and α is the QED fine structure constant. For the total cross section, it appears that these improved naïve exponentiation procedures are essentially adequate in $e^+e^- \to X$ at SLC and LEP energies.

However, in a realistic detector environment, such as that of the Mark II detector which will be operating at the SLC, one must consider the relevant detector cuts on the various final state phase space parameters. This necessitates an event-by-event analysis in which one rigorously includes the actual four-vectors in the production of multiple photons which, for example, generate the real infrared singularities, whose exponential cancellation[6] is responsible for the softening of the infrared singularity in the respective bremsstrahlung spectrum. Accordingly, we (together with Prof. S. Jadach) have developed a new approach[1,2,7] to $SU_{2L} \times U_1$ radiative corrections at high energies based on the Monte Carlo realization of the classic method of Yennie, Frautschi and Suura[6] for the summing and exponential cancellation of infrared contributions

to physical processes in Abelian gauge theories with massless gauge particles. The level of precision ultimately desired in the SLC–LEP type physics scenario will also require that the large ultraviolet (UV) logarithms are summed[1] (at least partially). We do this with the Weinberg–'t Hooft renormalization group equation.[1,2,8] It is this renormalization group improved Yennie–Frautschi–Suura theory which is the basis of our new approach to $SU_{2L} \times U_1$ radiative correction theory at high energies.

Similarly, the precise measurement of structure functions at HERA will necessitate high precision $SU_{2L} \times U_1$ radiative corrections. We call attention to the recent work of Kripfganz and Möhring,[9] wherein it is shown that the order α^3 (one-loop) $SU_{2L} \times U_1$ radiative corrections to $e + p \to e + X$ at HERA are x_{B_j}–dependent and $\lesssim 40\%$ in magnitude (this depends on cuts). Here, x_{B_j} is the famous Bjorken scaling variable $Q^2/2m_p\nu$, where $-Q^2$ is the square of the four-momentum transfer q from the incoming e^- to the p, $\nu = Q \cdot P_p/m_p$, and m_p is the proton rest mass. P_p is the initial proton four-momentum. Thus, high precision on these corrections necessarily involves summing the large infrared effects and, again, at least a partial summation of the large UV effects. Our renormalization group improved Yennie–Frautschi–Suura theory appears ideally suited for this case, also. Indeed, some preliminary work in this direction has already begun.[10] We hope to report elsewhere on this application of our ideas in the not-too-distant future.

Evidently, the physics output of the TLC and CLIC will also be greatly facilitated by precision $SU_{2L} \times U_1$ radiative corrections. The application of the Monte Carlo realizations of our new approach to $SU_{2L} \times U_1$ radiative corrections to such scenarios will be taken-up elsewhere.

In what follows, we will illustrate our approach to $SU_{2L} \times U_1$ radiative corrections in the SLC–LEP type scenario. We shall do this by briefly reviewing the renormalization group improved Yennie–Frautschi–Suura theory[1,2,7] in the next section. In Sect. III, we describe the actual Monte Carlo realizations of our theory for $e^+e^- \to f\bar{f} + n(\gamma)$, $f \neq e$ and $e^+e^- \to e^+e^- + n(\gamma)$. In Sect. IV, we present some numerical results. Section V contains our summary remarks.

II. RENORMALIZATION GROUP IMPROVED YENNIE–FRAUTSCHI–SUURA THEORY

In this section, we wish to review briefly the elements of the renormalization group improved Yennie–Frautschi–Suura theory. This theory is described in detail in Refs. 1, 2 and 7. We give this review here in the interest of completeness.

Specifically, we recall that the typical infrared (IR) singularity of the type illustrated in Fig. 1 is characterized by contributions of size $(2\alpha/\pi)[\ell n(s/m_e^2) - 1]$ $\ell n(\sqrt{s}/2\bar{k}_0)$, where $\bar{k}_0$ is a typical detector resolution-type cutoff on any radiated photon energy in Fig. 1. The typical UV contribution from the radiative effects illustrated in Fig. 1 is of size $t \equiv (2\alpha/\pi)[\ell n(s/m_e^2) - 1]$. For $\sqrt{s} = M_{Z^\circ}$, $t \simeq .108$ and we see that we need to sum all orders in the large infrared effects and at least three loops in the large UV effects, in order to achieve $\lesssim .3\%$ accuracy on the $SU_{2L} \times U_1$ radiative corrections illustrated in Fig. 1; for the $\bar{k}_0$ cutoff can easily be such that the large infrared effects are of order one in each order of perturbation theory. It is for this reason that we have developed the synthesis of the Weinberg-'t Hooft renormalization group and the rigorous infrared summation theory of Yennie, Frautschi and Suura (YFS); the former sums the relevant large UV effects and the latter sums the large infrared effects. We refer to this synthesis as renormalization group improved Yennie–Frautschi–Suura theory.

For a process such as $e^+e^- \rightarrow X$, where (as we have illustrated in Fig. 2) X may be $X' + n(\gamma)$ for some state X', we first recall from Ref. 2 that the respective differential cross section may be represented by the classic YFS result (the kinematics is summarized in Fig. 2)

$$d\sigma = \exp\{2\alpha(\mathrm{Re}\, B + \tilde{B})\} \frac{1}{(2\pi)^4} \int d^4y \, \exp\{iy(p_e + p_{\bar{e}} - P_{X'}) + D\}$$

$$\times \left[\bar{\beta}_0 + \sum_{n=1}^{\infty} \frac{1}{n!} \int \left(\prod_{j=1}^{n} \frac{d^3k_j}{k_j} \exp\{-iyk_j\} \right) \bar{\beta}_n \right] dE_{X'} \, d^3P_{X'} \,, \tag{1}$$

where (here, m_γ is our photon mass infrared regulator)

$$
B = \frac{-i}{8\pi^3} \int \frac{d^4k}{(k^2 - m_\gamma^2 + i\varepsilon)} \left[-\left(\frac{-2p_e + k}{k^2 - 2kp_e + i\varepsilon} + \frac{-2p_{\bar{e}} - k}{k^2 + 2kp_{\bar{e}} + i\varepsilon} \right)^2 \right.
$$

$$
+ e_f \left(\frac{-2p_e - k}{k^2 + 2kp_e + i\varepsilon} + \frac{2p_f + k}{k^2 + 2kp_f + i\varepsilon} \right)^2 - e_f \left(\frac{-2p_e - k}{k^2 + 2kp_e + i\varepsilon} + \frac{2p_{\bar{f}} + k}{k^2 + 2kp_{\bar{f}} + i\varepsilon} \right)^2
$$

$$
- e_f \left(\frac{-2p_{\bar{e}} - k}{k^2 + 2kp_{\bar{e}} + i\varepsilon} + \frac{2p_f + k}{k^2 + 2kp_f + i\varepsilon} \right)^2 + e_f \left(\frac{-2p_{\bar{e}} - k}{k^2 + 2kp_{\bar{e}} + i\varepsilon} + \frac{2p_{\bar{f}} + k}{k^2 + 2kp_{\bar{f}} + i\varepsilon} \right)^2
$$

$$
\left. - e_f^2 \left(\frac{2p_f - k}{k^2 - 2kp_f + i\varepsilon} + \frac{2p_{\bar{f}} + k}{k^2 + 2kp_{\bar{f}} + i\varepsilon} \right)^2 \right] ,
$$

(2)

$$
2\alpha\tilde{B} = \frac{\alpha}{4\pi^2} \int\limits^{k \leq K_{\max}} \frac{d^3k}{(k^2 + m_\gamma^2)^{1/2}}
$$

$$
\left[-\left(\frac{p_{\bar{e}}}{p_{\bar{e}}k} - \frac{p_e}{p_ek} \right)^2 + e_f \left(\frac{p_f}{p_fk} - \frac{p_e}{p_ek} \right)^2 - e_f \left(\frac{p_{\bar{f}}}{p_{\bar{f}}k} - \frac{p_e}{p_ek} \right)^2 \right.
$$

(3)

$$
\left. - e_f \left(\frac{p_f}{p_fk} - \frac{p_{\bar{e}}}{p_{\bar{e}}k} \right)^2 + e_f \left(\frac{p_{\bar{f}}}{p_{\bar{f}}k} - \frac{p_{\bar{e}}}{p_{\bar{e}}k} \right)^2 - e_f^2 \left(\frac{p_{\bar{f}}}{p_{\bar{f}}k} - \frac{p_f}{p_fk} \right)^2 \right]
$$

$$
\equiv \int\limits^{k \leq K_{\max}} \frac{d^3k}{(k^2 + m_\gamma^2)^{1/2}} \tilde{S}(k) ,
$$

$$
D \equiv \int \frac{d^3k}{k} \tilde{S} \left[\exp\{-iyk\} - \theta \left(K_{\max} - k \right) \right]
$$

(4)

(note that $K_{\max}$ may be taken to be the maximum energy of an undetectable photon but also that Eq. (1) does not depend on $K_{\max}$), and the residual cross section $\bar{\beta}_n$ for the emission of n real photons is free of both real and virtual infrared divergences and is defined in Refs. 1, 2 and 6. Explicit formulae for B and $\tilde{B}$ may be found in

6

Refs. 1, 2 and 6, for example. The result (1) then exhibits the famous cancellation of infrared divergences to all orders in α; for (from Refs. 1, 2 and 6) it may be checked that $Re\,B + \widetilde{B}$ is free of infrared divergences.

As we have observed already in the Introduction, the result (1) does not address the probable large UV logarithms which may occur in $d\sigma$. To handle these effects, we have used the Weinberg–'t Hooft renormalization group[8] to obtain the respective renormalization group improved form of Eq. (1). In Refs. 1 and 2, we have found that the respective improvement of Eq. (1) may be represented by making the following replacements in (1):

$$B \;\rightarrow\; B\left[p_i(1),\, m_{iR}(\lambda)\right]$$

$$\widetilde{B} \;\rightarrow\; \widetilde{B}\left[p_i(1),\, m_{iR}(\lambda),\, \frac{K_{\max}}{\lambda}\right]$$

$$\bar{\beta}_n \;\rightarrow\; \widetilde{\bar{\beta}}_n \;\equiv\; \lambda^{2\bar{D}_{M^{(n)}}}\, \bar{\beta}_n\left[p_i(1),\, k_{oj},\, m_{iR}(\lambda),\, \alpha(\lambda),\, \mu\right]\left[\frac{e_R(\lambda)}{e_R(1)}\right]^{-2n} \qquad (5)$$

$$D \;\rightarrow\; D\left[p_i(1),\, m_{iR}(\lambda),\, \alpha(\lambda),\, \frac{K_{\max}}{\lambda}\right]\,,$$

where $k_j = \lambda k_{oj}$, $p_i(\lambda) \equiv \left(\lambda\sqrt{s_0}/2,\, \sqrt{\lambda^2 s_0/4 - m_i^2}\,\hat{z}_i\right)$, $\hat{z}_i$ is the direction of motion of particle i, $m_i =$ physical rest mass of particle i, $\lambda = \sqrt{s}/2m_\mu$ and $\sqrt{s_0} = 2m_\mu$, for example, $\bar{D}_{M^{(n)}}$ is the engineering dimension of the connected amplitude $M^{(n)}$ for the production of n real photons with the final state X', $m_{iR}(\lambda)$ is the running mass parameter of particle i and $\alpha(\lambda) = e_R^2(\lambda)/4\pi$, where $e_R(\lambda)$ is the respective running electric charge of a positron so that it satisfies[8] $(\lambda d/d\lambda)\,e_R(\lambda) = \beta[e_R(\lambda)]$, where $\beta(e_R)$ is the respective coefficient function which expresses the response of e_R to changes in the normalization scale μ. [We show in Eq. (5) only the improvement effects due to QED for the purposes of our illustration; for the complete $SU_{2L} \times U_1$ theory, analogous improvements due to the SU_{2L} coupling g_{WR} should also be taken into account. This will be discussed elsewhere.]

For definiteness, we remind the reader that the respective Green functions of a renormalizable field theory satisfy the equation

$$\left[\mu \frac{\partial}{\partial \mu} + \beta(g_R) \frac{\partial}{\partial g_R} - \gamma_\Theta \, m_R \frac{\partial}{\partial m_R} - \gamma_\Gamma \right] \Gamma = 0 \, , \tag{6}$$

in the Weinberg–'t Hooft formulation of the renormalization group, where we imagine that there are but one coupling g_R and one mass parameter m_R for simplicity; the coefficient functions β, γ_Θ and γ_Γ are computable in renormalized perturbation theory, so that they may be considered as known in our $SU_{2L} \times U_1$ case. Note also that $m_R(\lambda)$ satisfies $\lambda dm_R(\lambda)/d\lambda = -\{1 + \gamma_\Theta[g_R(\lambda)]\} m_R(\lambda)$ here, so that the running masses $m_{iR}(\lambda)$ in Eq. (5) also reflect the response of the mass parameters of our theory to changes in the normalization scale. In this way, we avoid any problems with mass singularities in taking the UV limit of our $SU_{2L} \times U_1$ theory. We have, indeed, arrived at a rigorous procedure for summing the large IR and UV effects to all orders in the respective couplings in $SU_{2L} \times U_1$ processes at high energies such as those typical of SLC and LEP.

We shall now turn to the Monte Carlo realizations of our procedure. This is the subject of the next section.

III. MONTE CARLO REALIZATIONS OF RENORMALIZATION GROUP–IMPROVED YENNIE–FRAUTSCHI–SUURA THEORY

The general recipe for applying (1)–(5) to a standard one-photon Monte Carlo event generator, such as the well-known MMG1 event generator[11] for $e^+e^- \rightarrow \mu^+\mu^-(\gamma)$, is described in detail in Refs. 1, 2 and 7. Recently, using this recipe, Jadach and the author[12] have succeeded in constructing event generators which realize (1)–(5) by the Monte Carlo method on an event-by-event basis so that, for the first time in $SU_{2L} \times U_1$ radiative correction simulations, the physical four-vectors of the multiple photon final states are produced among the list of the final state particle four-vectors. In this section we wish to discuss these multiple photon Monte Carlo event generators.

Specifically, the first Monte Carlo realization of our approach to $SU_{2L} \times U_1$ radiative correction theory has been achieved for the $\tau\bar{\tau}$ pair type production in $e^+e^- \to X$, for example, at SLC and LEP energies. The extension to $f\bar{f}, f = \mu, u, d, s, c, b$ and t is immediate, so that we will concentrate here on $\tau\bar{\tau}$ production for definiteness.

The recipe in Refs. 1, 2 and 7 is effected as follows for $e^+e^- \to \tau\bar{\tau} + n(\gamma)$. One rewrites (1) in the form[12]

$$d\sigma(s) = \sum_{n=0}^{\infty} \frac{1}{n!} \int_{k_\ell^o > K_{max}} d\tau_{n+2}'(P; q_1, q_2, k_1, \ldots, k_n) \left[\prod_{\ell=1}^{n} \widetilde{S}(k_\ell) \right] \tag{7}$$

$$b_n(q_1, q_2; k_1, \ldots, k_n)$$

where

$$b_n(q_1, q_2, k_1, \ldots, k_n) = \exp\{2\alpha(ReB + \widetilde{B})\} \left[\bar{\beta}_0(Rq_1, Rq_2) + \sum_{j=1}^{n} \frac{\bar{\beta}_1(Rq_1, Rq_2, k_j)}{\widetilde{S}(k_j)} \right]. \tag{8}$$

Here, the following definitions have been used: $P = p_e + p_{\bar{e}}$, where $p_{e(\bar{e})}$ is the four-momentum of the incoming $e^-(e^+)$ so that $q_{1(2)}$ is the four-momentum of the outgoing $\tau(\bar{\tau})$,

$$d\tau_n'(P; \bar{p}_1, \ldots, \bar{p}_n) = \left(\prod_{i=1}^{n} \frac{d^3\bar{p}_i}{\bar{p}_i^o} \right) \int \frac{d^4y}{(2\pi)^4} \exp\left\{ iy \left(P - \sum_{i=1}^{n} \bar{p}_i \right) + D \right\}, \tag{9}$$

and Rq_i are the respective reduced four-momenta[12] which are such that $\bar{\beta}_i$ are evaluated at the appropriate infrared point for the multiparticle state with four-momenta $(q_1, q_2, k_1, \ldots, k_n)$; i.e., the R operation allows $q_1 + q_2 + \sum_i k_i = P$ to be transformed into $Rq_1 + Rq_2 = P$ for the $\bar{\beta}_0$ terms included in (7), for example, and it is implicit in the YFS theory; we discuss it more explicitly in Ref. 12.

The expression (7) is now primed for Monte Carlo methods. Specifically, focussing on the famous Bonneau–Martin[13] type problem for $\tau\bar{\tau}$ pair production, we use the recipe in Refs. 1, 2 and 7 to extract the respective $\bar{\beta}_0$ and $\bar{\beta}_1$. We write[12,14] the

Bonneau–Martin cross section [here, $\delta_{SX}(x_o) \equiv (\alpha/\pi)\left\{(3/2)\ell n(s/m_e^2) - 2 + \pi^2/3\right\} + (2\alpha/\pi)\left\{\ell n(s/m_e^2) - 1\right\}\ell n\, x_0$ and $x_0\sqrt{s}/2 \equiv K_{max}$] as

$$\sigma_{BM}(s) = \sigma^B(s)\left[1 + \delta_{SX}(s/m_e^2, x_0)\right]$$

$$+ \int\limits_{x_0}^{1} \frac{dx}{x} \int d\Omega_\gamma \left[\int d\Omega_1\, g_1(x, \cos\theta_\gamma)\, \frac{d\sigma^B}{d\Omega_1}\, (s', \cos\theta_1)\right.$$

$$\left. + \int d\Omega_2\, g_2(x, \cos\theta_\gamma)\, \frac{d\sigma^B}{d\Omega_2}\, (s', \cos\theta_2)\right], \tag{10}$$

where superscript B denotes the Born approximation and where the final fermion directions $d\Omega_i, i = 1, 2$, correspond to two choices of the z-axis in the rest frame of the final fermions (rcms): for $i = 1$, it points in the direction of the first beam and for $i = 2$, it points opposite to the direction of the second beam. The g_i are defined as follows:

$$g_i(x, \cos\theta_\gamma) = \frac{\alpha}{2\pi^2}\left(1 - \frac{1}{2}x\delta_i\right)^2\left[\frac{1}{\delta_1\delta_2} - \frac{2m_e^2}{s}\frac{1 - x}{1 + (1 - x)^2}\left(\frac{1}{\delta_1^2} + \frac{1}{\delta_2^2}\right)\right],$$

$$\tag{11}$$

$$\delta_1 = 1 - \cos\theta_\gamma\sqrt{1 - 4m_e^2/s}, \qquad \delta_2 = 1 + \cos\theta_\gamma\sqrt{1 - 4m_e^2/s}.$$

(Here, x_0 provides the usual separation between hard and soft real photons and $s' = (1 - x)s$.) It can be shown that Eqs. (10) and (11) do indeed represent the Bonneau–Martin formula for $\tau\bar{\tau}$ production.

From Eqs. (10) and (11), one arrives at the following expressions for $\bar{\beta}_0$ and $\bar{\beta}_1$:[12]

$$\bar{\beta}_0(q_1, q_2) = \frac{d\sigma^B}{d\tau_2(P; q_1, q_2)}\,(1 + 2ReF_1 - 2Re\alpha B)$$

$$\tag{12}$$

$$= \frac{2}{\beta'}\frac{d\sigma^B}{d\Omega}\,(s, \cos\theta)\left[1 + \frac{\alpha}{\pi}\left(\ell n\frac{s}{m_e^2} - 1\right)\right],$$

where $\beta' = (1 - 4m_f^2/s)^{1/2}$, $d\tau_2 = d\tau_2'|_{D=0}$ and

$$\frac{\bar{\beta}_1(q_1, q_2, k)}{\widetilde{S}(k)} = \frac{2}{\beta'} \left\{ \frac{g_1(x, \cos\theta_\gamma)}{g_0(x, \cos\theta_\gamma)} \frac{d\sigma^B}{d\Omega}(s', \cos\theta_1) + \frac{g_2(x, \cos\theta_\gamma)}{g_0(x, \cos\theta_\gamma)} \frac{d\sigma^B}{d\Omega}(s', \cos\theta_2) \right.$$
$$\left. - \frac{1}{2} \left[\frac{d\sigma^B}{d\Omega}(s, \cos\theta_1) + \frac{d\sigma^B}{d\Omega}(s, \cos\theta_2) \right] \right\},$$

$$(13)$$

where

$$g_0(x, \cos\theta_\gamma) = \frac{\alpha}{2\pi^2} \left[\frac{1}{\delta_1 \delta_2} - \frac{m_e^2}{s} \left(\frac{1}{\delta_1^2} + \frac{1}{\delta_2^2} \right) \right] \qquad (14)$$

is up to a normalization constant equal to the initial state restriction of $\widetilde{S}(k)$. In the last two terms in (13), we have effected the respective R procedure as it is explained in detail in Ref. 12. We note that, using entirely analogous procedures, we have also constructed the leading logarithmic approximation to $\bar{\beta}_2$.

The actual Monte Carlo algorithm proceeds as follows. We generate events according to our formula (7) with a simplified b_n function, b_n', and algorithm No. 2 in Ref. 7 (the latter algorithm is also described in detail in Ref. 2). Here,

$$b_n'(q_1, q_2, k_1, \ldots, k_n) = \frac{1}{2\pi\beta'} \sigma^B \left((q_1 + q_2)^2 \right) \quad . \qquad (15)$$

The real distribution is then recovered using the standard rejection method with weight

$$w = \frac{b_n'}{b_n} \, . \qquad (16)$$

It is in this way that Jadach and the author have realized (7) on an event-by-event basis for $e^+e^- \rightarrow \tau\bar{\tau} + n(\gamma)$ and, more recently,[15] in the luminosity monitor region in $e^+e^- \rightarrow e^+e^- + n(\gamma)$ at SLC and LEP energies. The two respective FORTRAN programs are YFS FORTRAN and BHLUMI FORTRAN; they are available from Jadach and the author upon request and they will be described in detail elsewhere.

We will now present some results which we have derived from our Monte Carlo realizations of Eq. (7). This is the subject of the next section.

IV. NUMERICAL RESULTS

In this section, we wish to illustrate the type of results which we have obtained from our Monte Carlo realizations of Eq. (7) at SLC and LEP energies. We begin with the $\tau\bar{\tau}$–pair type of process.

Specifically, as we have indicated, we have currently a realization of Eq. (7) for $\tau\bar{\tau}$–pair production in which all initial state multiple photon emission effects are taken into account. It is then of interest to compare our YFS procedure to the various other approaches[3,5] to initial and final state radiative effects in e^+e^- annihilation into $\tau\bar{\tau}$–pairs. We do this comparison in Fig. 1, where we show the respective Born cross section, the cross section from the Bonneau–Martin formula, and the naïve exponentiation ansatz of Jackson and Scharre, and the more modern realization of Jackson and Scharre's ideas as represented by the Kuraev–Fadin formula in the caption in Fig. 3. A detailed comparison of the modern realizations of the Jackson–Scharre ideas may be found in Ref. 5. (We may now explicitly note the principal improvements over the original work of Jackson and Scharre by a Kuraev–Fadin type formula: namely, in the original work, the approximation is made that the higher order corrections represented by the δ_R in the caption in Fig. 3 only affect the cross section at $x = 0$ whereas, in the Kuraev–Fadin type formula, the entire Jackson–Scharre kernel tx^{t-1} is renormalized by δ_R. See Refs. 3 for more discussion of this point. Related work by Cahn and Greco in Refs. 3 may also be of interest here.) The results of the YFS FORTRAN Monte Carlo are represented by the dots. They are obtained from samples of 10^4 events so that the statistical error is the size of the dot. We show at each energy two possible upper limits on the energy of the soft photon E_γ^{soft}. There is no limit on the energy of the most energetic photon but all other ones must stay below $\bar{E}_\gamma^{soft}$, where $\bar{E}_\gamma^{soft} = 0.1$ GeV corresponds to the lower cross section. We note that the result of the Monte Carlo is close to that of the Kuraev–Fadin formula and that the dependence of the Monte Carlo result on $\bar{E}_\gamma^{soft}$ is a weak one. This dependence, however, is essential.

The crosses in Fig. 3 show the effects of renormalization group improvement, via Eq. (5), of the cross section represented by the round dots in Fig. 3. We see that these effects are significant if one wants high precision Monte Carlo simulations—precision

of the type relevant for the SLC–LEP objectives.

Turning next to the luminosity monitor regime for $e^+e^- \to e^+e^- + n\gamma$, we have in mind the MINISAM type scenario, where 15.2 mrad $\leq \theta_{cm}(\bar{e}) \leq$ 25 mrad, 16.2 mrad $\leq \theta_{cm}(e) \leq$ 24.5 mrad for the usual center of momentum scattering angles $\theta_{cm}(f)$, $f = e, \bar{e}$. We presume full azimuthal sensitivity, we require the acollinearity to be less than $10°$, and we require that the sum of E'_e and $E'_{\bar{e}}$ exceeds .6 of $\sqrt{s}$ in the c.m. system. Here, E'_f is the energy of f in the respective final state. We show in Fig. 4 the YFS Monte Carlo type results generated by BHLUMI FORTRAN on the basis of Eq. (7) as the round dots in the figure. For comparison, we also show the analogous results generated by the conventional Berends–Kleiss[16] type of one real photon Monte Carlo. We see that near the $Z°$, in order to achieve the highest precision in the MINISAM cross section, multiple photon effects should be taken into account. Again, the statistical error is the size of the dot.

We feel, therefore, that the way to realistic event-by-event multiphoton radiative corrections at high energies is now open. The results in this section support the idea that such an approach to radiative corrections is appropriate for high precision checks of the $SU_{2L} \times U_1$ standard electroweak theory.

V. CONCLUSIONS

What we have shown in this discussion is that renormalization group improved Yennie–Frautschi–Suura theory provides a rigorous method of achieving $\leq 1\%$ radiative corrections in the $SU_{2L} \times U_1$ theory of electroweak interactions at high energies. We have illustrated this with Monte Carlo data which realize, on an event-by-event basis, the effects of multiple photon emission as prescribed by the YFS theory.

Indeed, we have shown that the way to subtle checks of the $SU_{2L} \times U_1$ theory is open. Our event generators for $e^+e^- \to f\bar{f} + n(\gamma), f \neq e$, and $e^+e^- \to e^+e^- + n(\gamma)$

allow one to study in detail $P_\perp$ effects, the effects of detector cuts on A_{FB} and A_{LR}, the $f\bar{f}$ energy, and further effects. Such phenomena will be taken up elsewhere.

We are very much encouraged by what we have found. We look forward with enthusiasm to the application of our approach to $SU_{2L} \times U_1$ radiative corrections to actual high energy interactions at SLC, LEP, HERA, TLC, CLIC and elsewhere. This is not far off.

ACKNOWLEDGMENTS

REFERENCES

1. See, for example, B. F. L. Ward, Acta. Phys. Pol. **B19**, 465 (1988); P. Rankin, *Proceedings of the Mark II SLC Pajaro Dunes Workshop*, ed. J. Hu (SLAC, Stanford, CA, 1987); G. Altarelli, *Physics at LEP*, eds. J. Ellis and R. Peccei (CERN, Geneva Switzerland, 1985), G. Altarelli, *Proceedings of the HERA Experiments*, (Genoa, Italy, 1984); G. Altarelli, *Proceedings of the La Thuile Workshop 1987, Vol. 1*, ed. J. H. Mulvey (CERN, Geneva, Switzerland, 1987); and references therein.

2. See, for example, B. F. L. Ward, Phys. Rev. **D36**, 939 (1987) and references therein.

3. E. A. Kuraev and V. S. Fadin, Sov. J. Nucl. Phys. **41**, 466 (1985); F. Berends et al., Phys. Lett. **185B**, 395 (1987); O. Nicrosini and L. Trentadue, preprint FNT/T–87/17, 1987; R. N. Cahn, Phys. Rev. **D36**, 2666 (1987); M. Greco, preprint LNF–86/55–P–Rev., 1987; G. Altarelli and G. Martinelli, *Physics at LEP*, eds. J. Ellis and R. Peccei (CERN, Geneva, Switzerland, 1985); B. W. Lynn *et al.*, SLAC–PUB–4128, 1988 and references therein.

4. J. D. Jackson and D. L. Scharre, Nucl. Instrum. Methods **128**, 13(1975).

5. J. P. Alexander *et al.*, Phys. Rev. **D37**, 56 (1988).

6. D. R. Yennie, S. C. Frautschi and H. Suura, Annals of Phys. **13**, 379 (1961).

7. S. Jadach, preprint of Max–Planck–Institut München, MPI–PAE/PTh6/87.

8. S. Weinberg, Phys. Rev. **D8**, 3497 (1973); G. 't Hooft, Nucl. Phys. **B61**, 455 (1973).

9. J. Kripfganz and H. J. Möhring, preprint DESY 87–139, 1987.

10. S. Jadach, preprint of Max–Planch–Institut München, MPI–PAE/PTh75/86.

11. F. A. Berends, R. Kleiss and S. Jadach, Comp. Phys. Comm. **29**, 185 (1983).

12. S. Jadach and B. F. L. Ward, SLAC–PUB–4543, 1988, in press at Phys. Rev. D; preprint UTHEP–88–0201, 1988.

13. G. Bonneau and J. Martin, Nucl. Phys. **B27**, 381 (1971).

14. F. A. Berends and R. Kleiss, Nucl. Phys. **B177**, 237 (1981).

15. S. Jadach and B. F. L. Ward, to appear.

16. F. A. Berends and R. Kleiss, Nucl. Phys. **B228**, 537 (1983).

FIGURE CAPTIONS

1. Radiative corrections to $e^+e^- \to X$.

   (a) Virtual infrared divergence

   (b) Real infrared divergence.

2. Multiple photon emission in $e^+e^- \to X$, $X = X' + n(\gamma)$.

3. Two solid curves represent the Born and Bonneau–Martin cross sections. The dotted curve is according to Jackson–Scharre and the dashed curve is from the Kuraev–Fadin result.[a] Three types of points come from our Monte Carlo, 10^4 events, statistical error below the size of the dots. Round and square dots represent the Monte Carlo result for $\bar\beta_0 + \bar\beta_1 + \bar\beta_2$ and triangle points represent the $\bar\beta_0 + \bar\beta_1$ result. The most energetic photon is allowed everywhere in the phase space, and the other photons are confined within a sphere $E_\gamma < \bar E_\gamma^{soft}$. Two values for the $\bar E_\gamma^{soft}$ cutoff are used: 2 GeV and 0.1 GeV. The crosses show the effect of renormalization group improvement on the round dots.

   [a]The Kuraev–Fadin result is defined as follows:

$$\sigma_{KF} = \int\limits_0^1 dx \sigma^B\left[s(1-x)\right]\left[\alpha A x^{\alpha A - 1}(1 + \delta_R) + \alpha A\left(-1 + \frac{x}{2}\right)\right] ,$$

$$\delta_R = \frac{3}{2}\frac{\alpha}{\pi}\left[\ell n\frac{s}{m_e^2} - 1\right] + \frac{\alpha}{\pi}\left(\frac{\pi^2}{3} - 2\right) ,$$

$$\alpha A = \frac{2\alpha}{\pi}\left[\ell n\frac{s}{m_e^2} - 1\right] = t \quad .$$

4. Luminosity monitor results for $\sqrt{s} \sim M_{Z^o}$: the dots represent our multiple photon Monte Carlo result for $\bar\beta_0 + \bar\beta_1$; the crosses represent the one-photon Monte Carlo result of Berends and Kleiss.[16] The statistical error is the size of the dot. The monitor configuration is that of the MINISAM of the MARK II at the SLC: 16.2 mrad $\leq \theta_{cm}(e) \leq$ 24.5 mrad, 15.2 mrad $\leq \theta_{cm}(\bar e) \leq$ 25 mrad, where

$\theta_{cm}(f)$ is the respective c.m. scattering angle of f, $f = e, \bar{e}$; $E'_e + E'_{\bar{e}} > .6\sqrt{s}$ in the c.m. system, and acollinearity $< 10°$, where E'_f is the final state energy of f, $f = e, \bar{e}$.
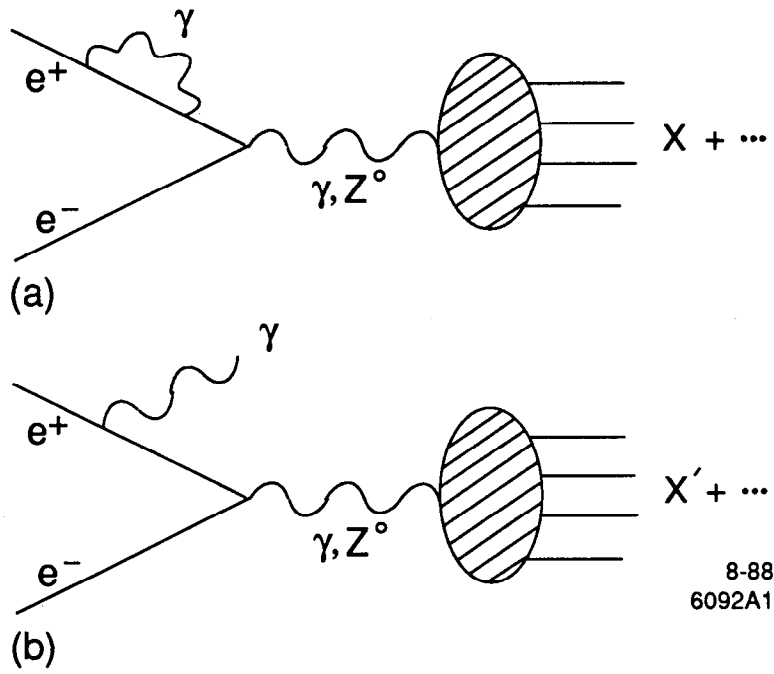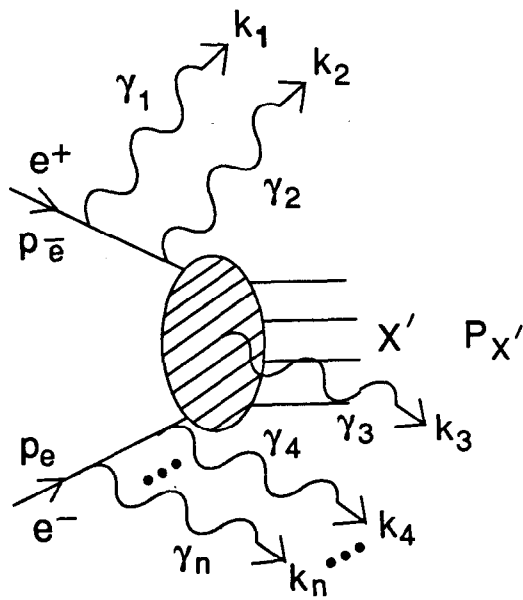
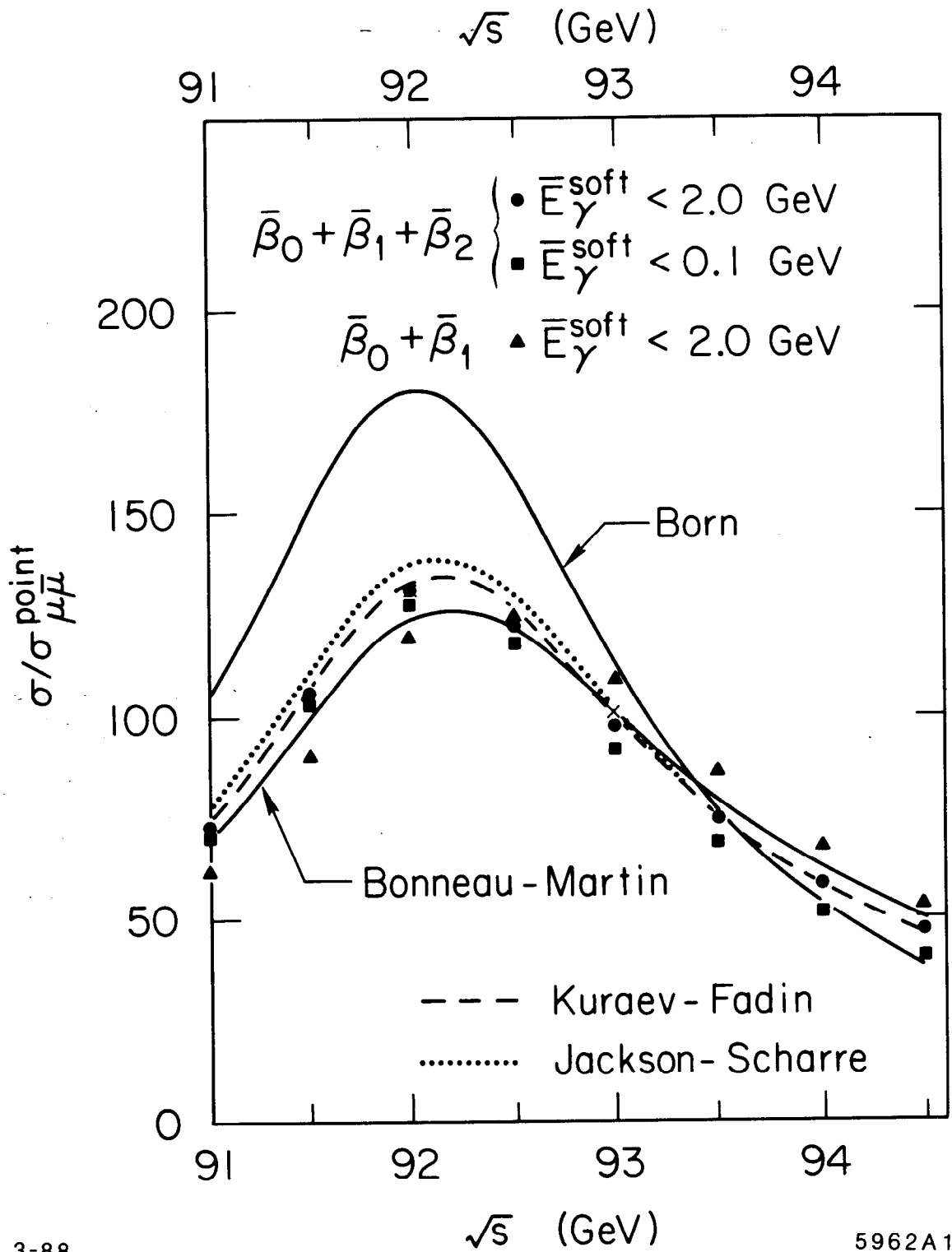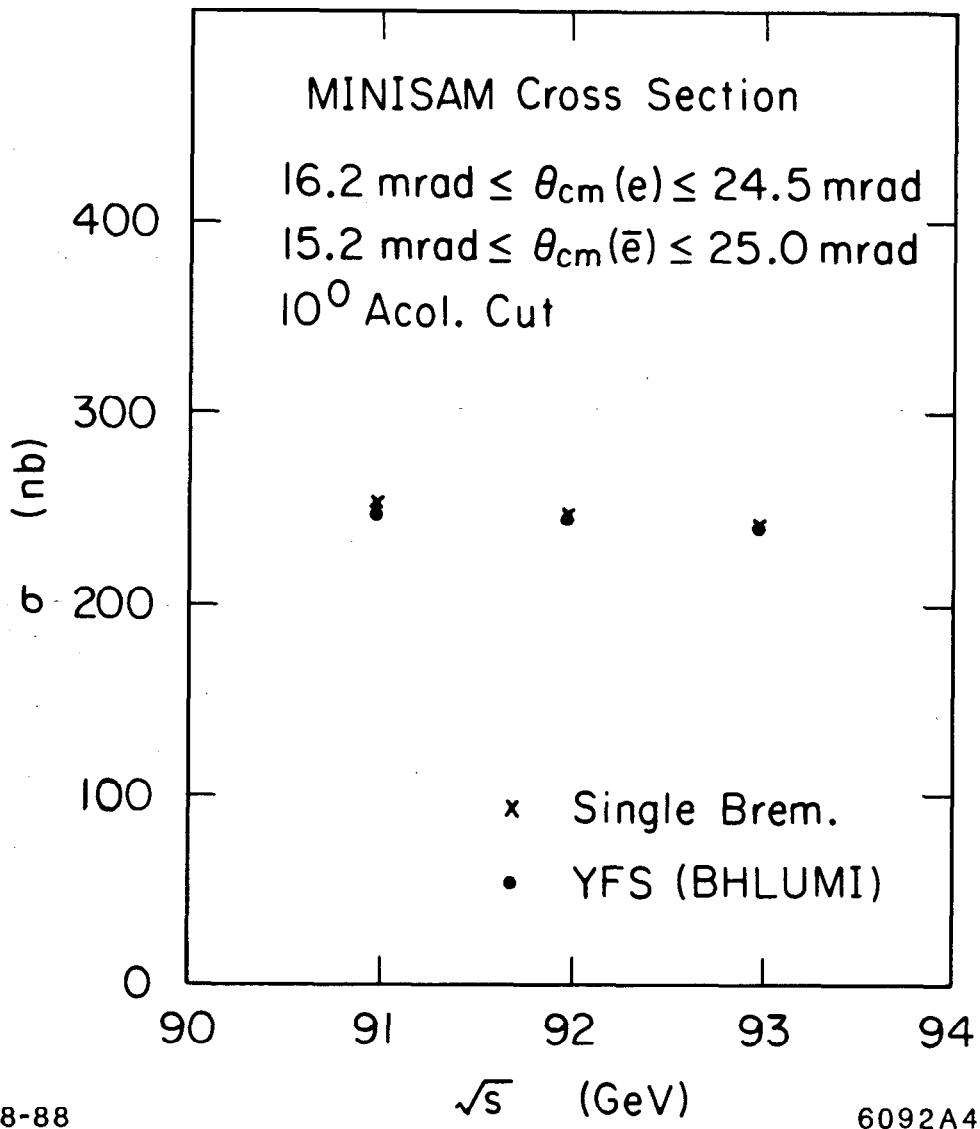Fig. 1

Fig. 2

8-88
6092A2

Fig. 3

MINISAM Cross Section

$16.2 \text{ mrad} \leq \theta_{cm}(e) \leq 24.5 \text{ mrad}$
$15.2 \text{ mrad} \leq \theta_{cm}(\bar{e}) \leq 25.0 \text{ mrad}$
10^0 Acol. Cut

x   Single Brem.

•   YFS (BHLUMI)

8-88   6092A4

Fig. 4